Polarimetric Response and Calibration of a Single Stand Embedded in an Array with Irregular Wavelength-Scale Spacings

Steve Ellingson*

August 14, 2008

Contents

*Bradley Dept. of Electrical & Computer Engineering, 302 Whittemore Hall, Virginia Polytechnic Institute & State University, Blacksburg VA 24061 USA. E-mail: ellingson@vt.edu

1 Summary

LWA Memo 138 [1] addressed the polarimetric response and calibration of an LWA antenna stand in the absense of any other antenna elements. This memo repeats portions of this analysis for the case in which the stand is located near the center of the proposed LWA station consisting of a pseudorandom arrangement of identical stands. In this memo, the single-stand scenario is referred to as "standalone stand" and array scenario is referred to as "embedded stand." Only the new results are presented here; for assumptions and details of the analysis please refer to [1].

New findings are as follows:

- The self-impedance of the embedded stand is different from that of the standalone stand by no more than a few percent in magnitude and phase over most of the frequency range of interest. The exception is near first resonance, where large differences are possible because the self-impedance is changing rapidly with frequency in this region. In general, the difference is greatest at the high end of the frequency range and negligible below first resonance.
- For zenith pointing, the dispersion and calibratibility of the embedded stand is not significantly different from that of the standalone stand.
- The above result also pertains to low-elevation pointing, however the resulting performance is slightly different, although not significantly worse.

2 Results

The design of the antenna stand is in all respects identical to that described in LWA Memo 138 [1], except that now we assume that in the "embedded stand" case the stand is centrally-located in the array geometry shown in Figure 1. This geometry was derived from a 256-stand, 100-meter diameter design originally developed by NRL which optimizes the sidelobe levels in the absense of mutual coupling, subject to a 4-meter minimum spacing constraint. To reduce the computing effort to a reasonable level, only the 63 stands closest to the stand being considered are included in the electromagnetic (NEC2) model. An infinite perfectly-conducting ground plane is assumed.

The "standalone stand" case is generated simply by scaling the $x - y$ dimensions of the array by a factor of 100, leaving the stand design itself unaltered. The assumption is that the behavior of the stand being considered is not affected by the presense of other stands, which are all at least 400 m distant in this case.

Figure 2 compares the antenna self-impedance for the embedded and standalone cases. Note that the self-impedance of the embedded stand is different from that of the standalone stand by no more than a few percent in magnitude and phase over most of the frequency range of interest. The exception is near first resonance, where large differences are possible because the self-impedance is changing rapidly with frequency in this region. In general, the difference is greatest at the high end of the frequency range and negligible below first resonance.

Figures 3 and 4 show the response at the far end of the cable to a signal incident from the zenith for the embedded and standalone cases, respectively. The cable of course results in further frequency-dependent reduction of the voltage (through attenuation), and increases the apparent dispersive delay. Note that the difference between the embedded and standalone results is very small.

Figures 5 and 6 show the frequency response after conversion to circular polarization and calibration using $M = 16$ tap FIR filters, for the embedded and standalone cases, respectively. As expected, the difference is very small.

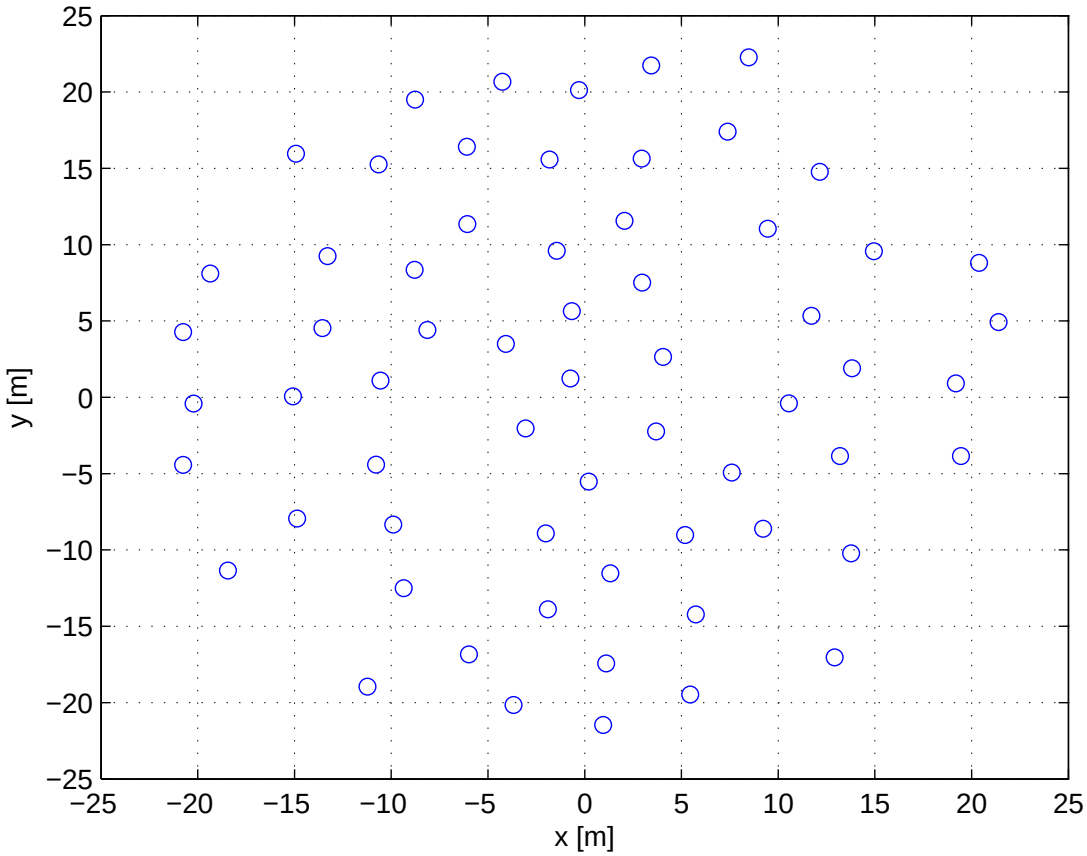

Figure 1: Station array geometry used in this study. The circles denote the stand locations. The stand being evaluated is the one closest to (slightly left and above) the origin.

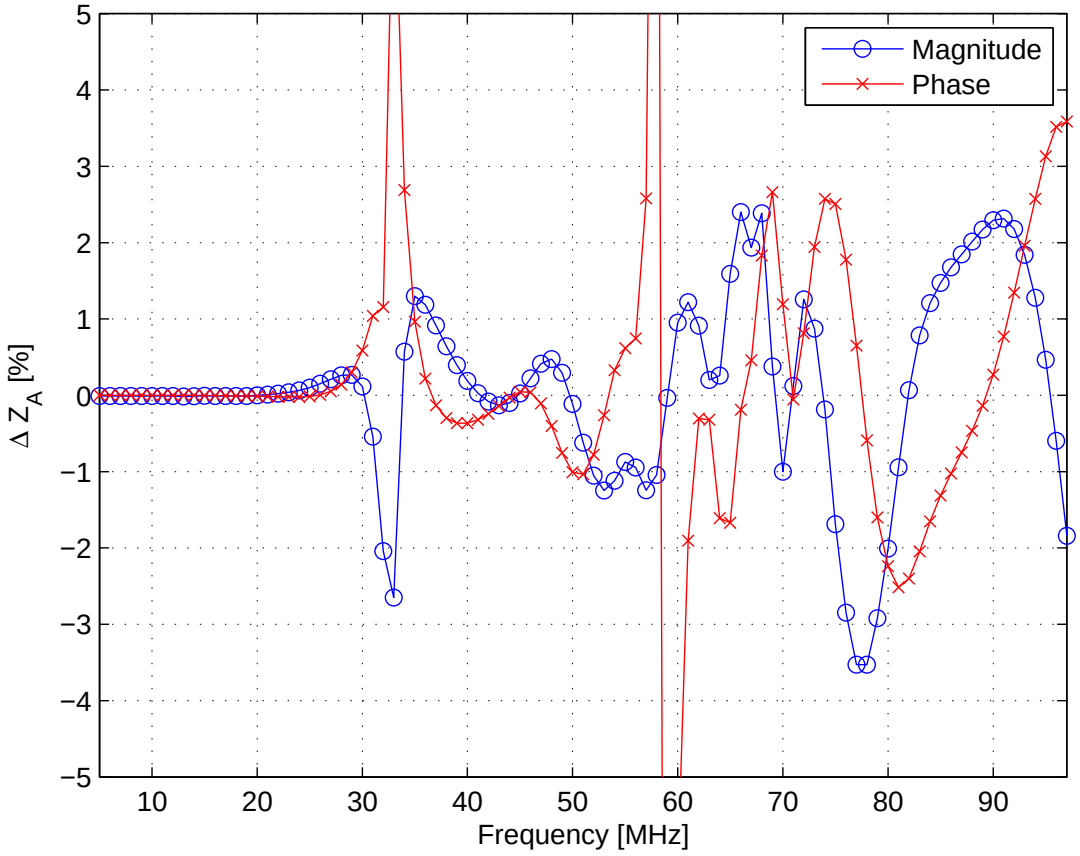

Figure 2: Difference between the self-impedance of (1) the antenna in the original array ("embedded") and (2) the same antenna when the array spacings are scaled up by 100 ("standalone").

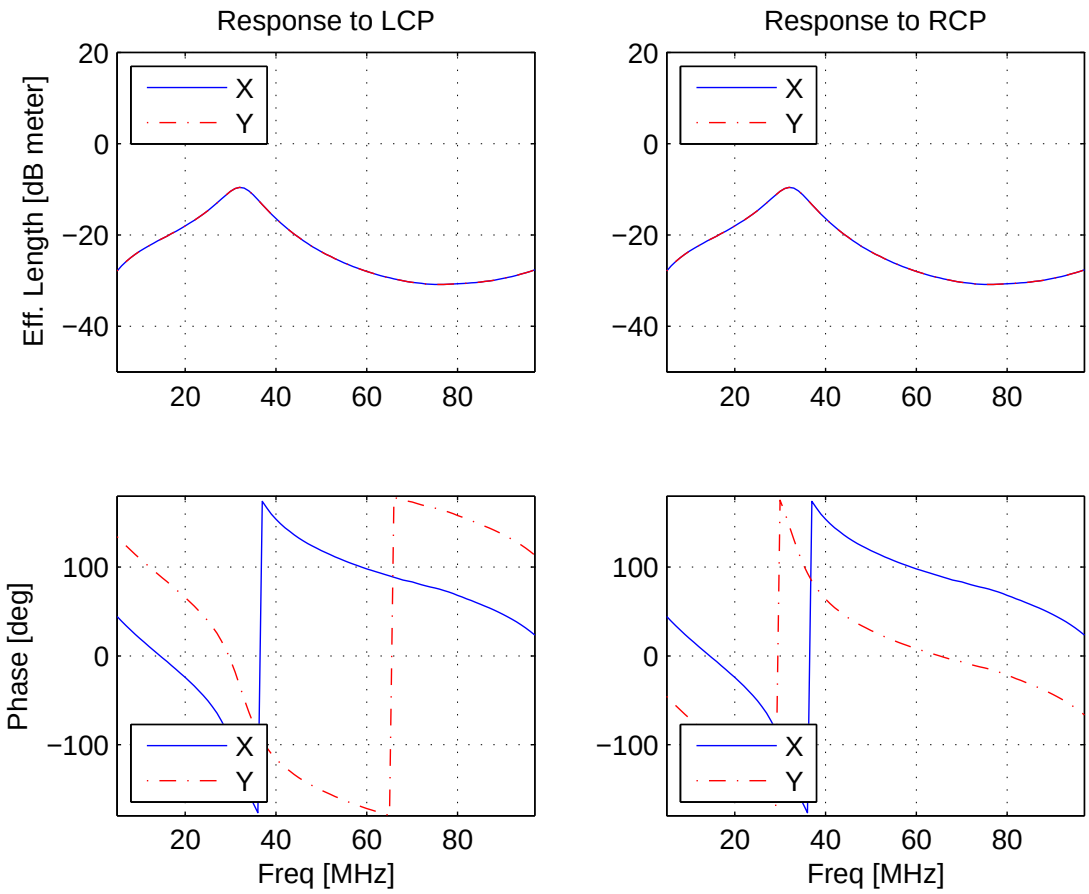

Figure 3: Zenith incidence, cable output, embedded stand.

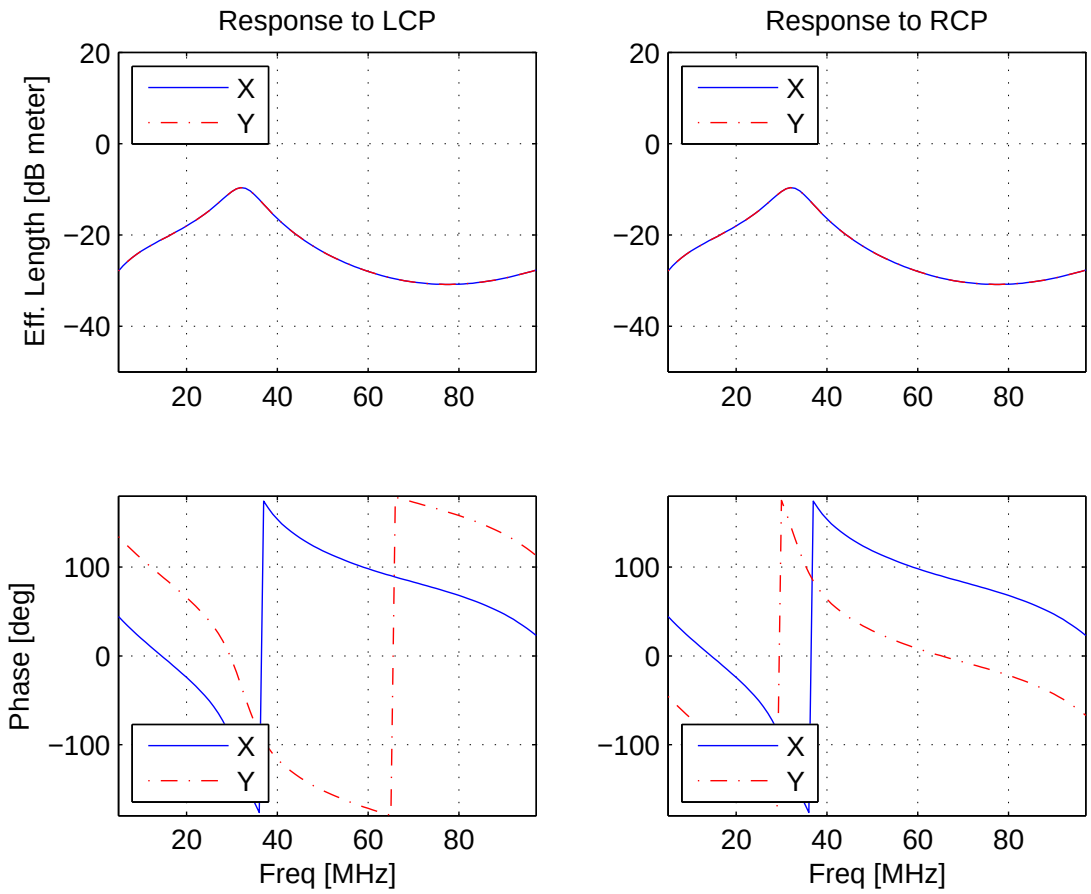

Figure 4: Zenith incidence, cable output, standalone stand.

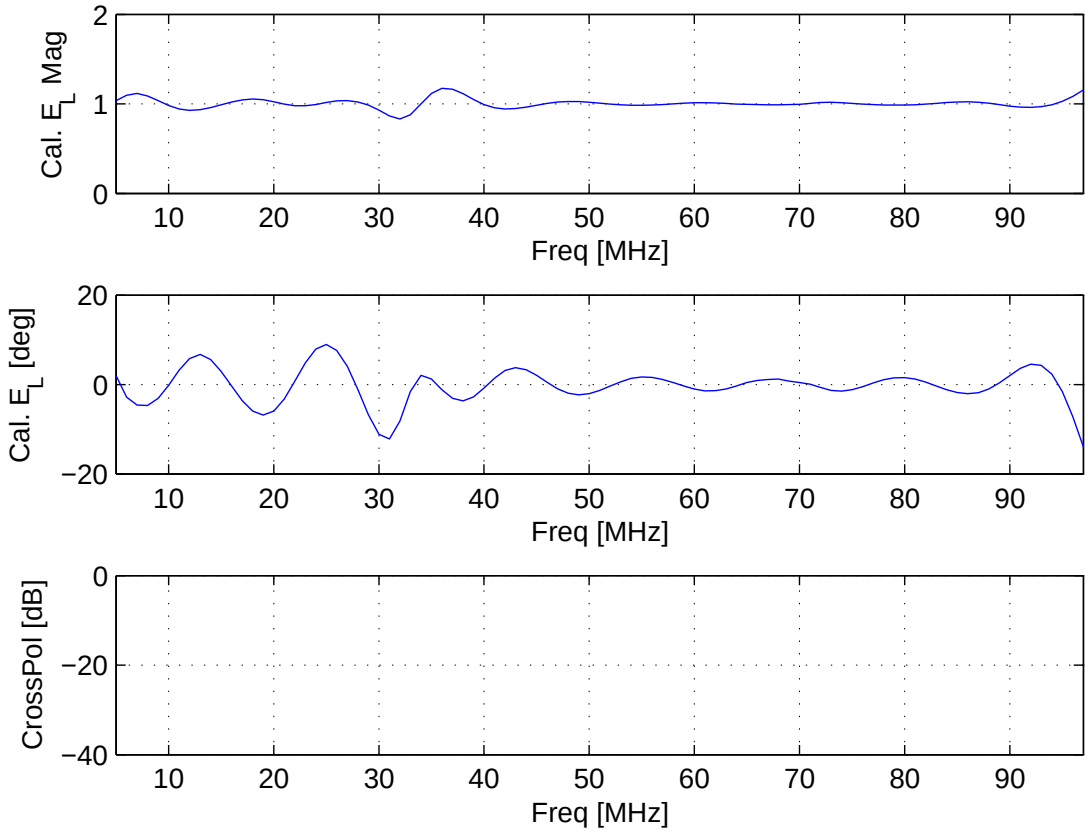

Figure 5: Zenith incidence, cable output, embedded stand.

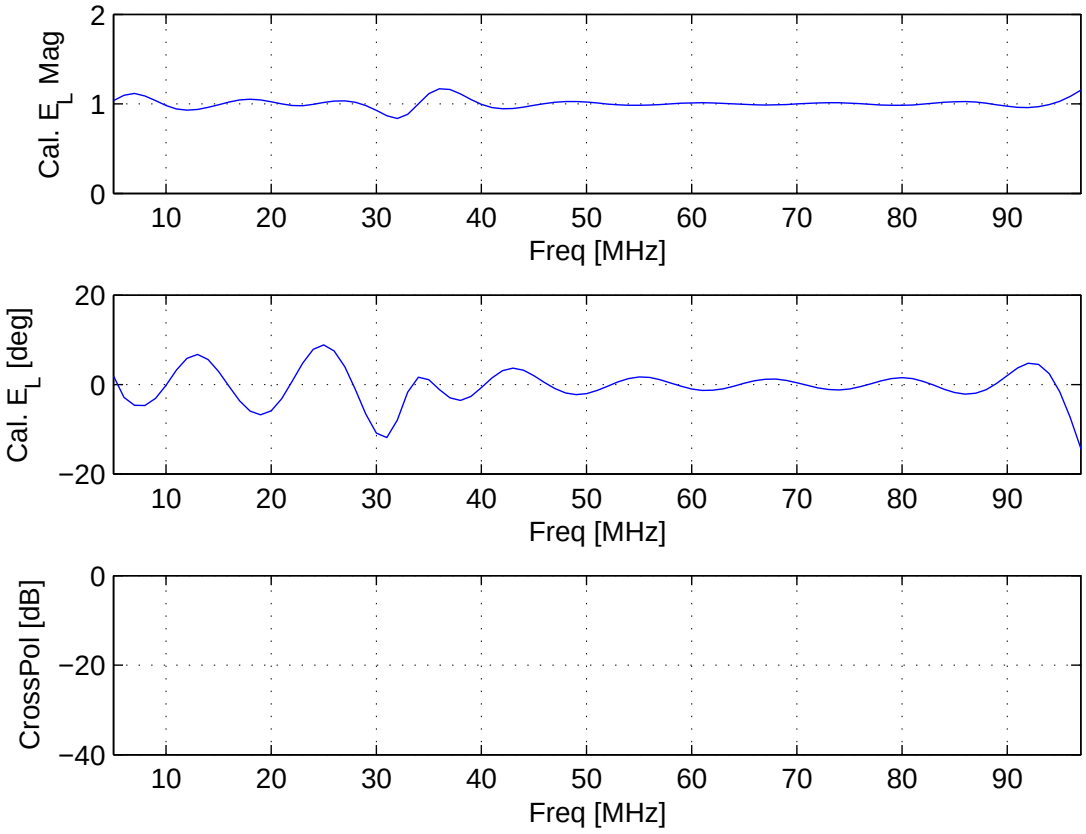

Figure 6: Zenith incidence, cable output, standalone stand.

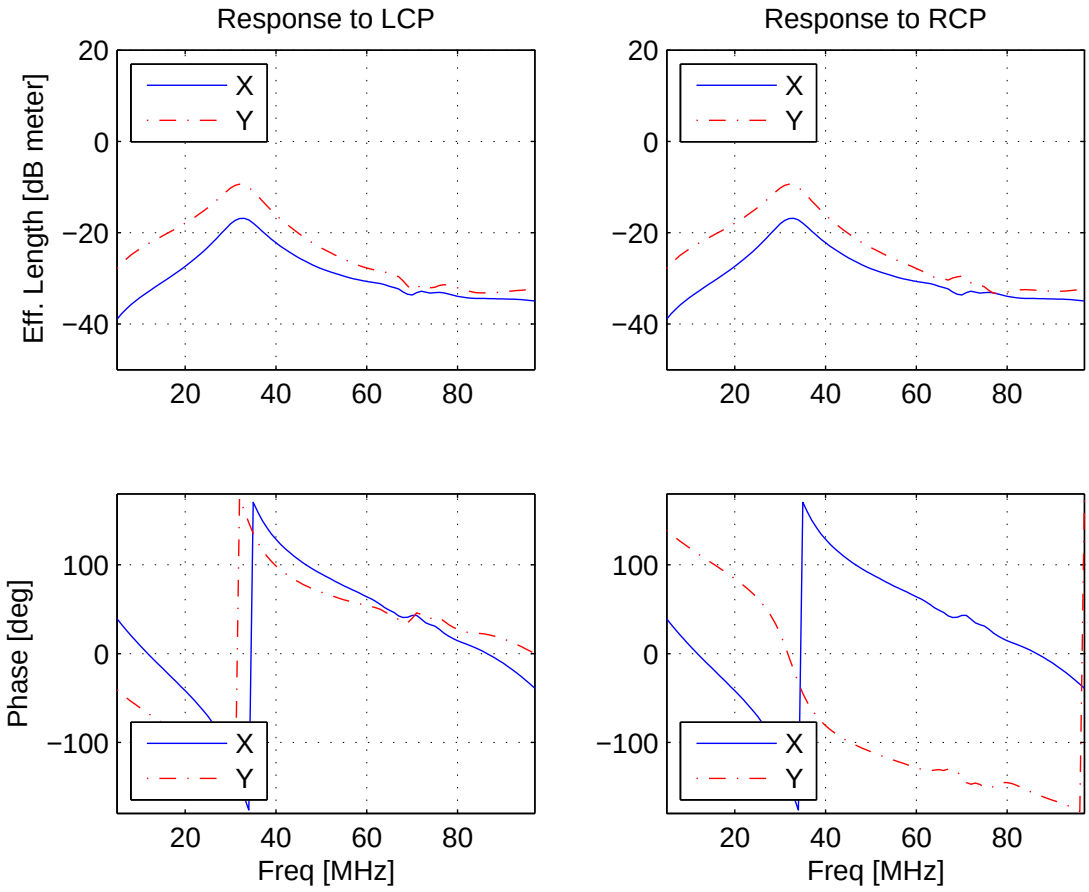

Figure 7: $\theta = 74°$, $\phi = 0$, embedded stand.

Figures 7 and 8 show the response at the far end of the cable to a signal incident from zenith angle 74° in the E-plane for the embedded and standalone cases, respectively. Note that the difference between the embedded and standalone results is very small, although a new "glitch" around 70 MHz has appeared. It may or may not be coincidence that the wavelength associated with this frequency corresponds to the minimum spacing between stands in the array; future study should consider this. It should be noted that it is not certain that this feature exists in practice; future study should consider the possibility that this is a artifact of the analysis technique. These analyses are fairly straightforward but tedious tasks.

Figures 9 and 10 show the frequency response after conversion to circular polarization and calibration using $M = 16$ tap FIR filters, for the embedded and standalone cases, respectively. Once again, the difference is very small.

Figures 11 and 12 show the response at the far end of the cable to a signal incident from zenith angle 74° in the diagonal plane (i.e., half-way between the E- and H-planes) for the embedded and standalone cases, respectively. Note that the difference between the embedded and standalone results is very small, although the 70 MHz "glitch" is becoming more prominent.

Figures 13 and 14 show the frequency response after conversion to circular polarization and calibration using $M = 16$ tap FIR filters, for the embedded and standalone cases, respectively.

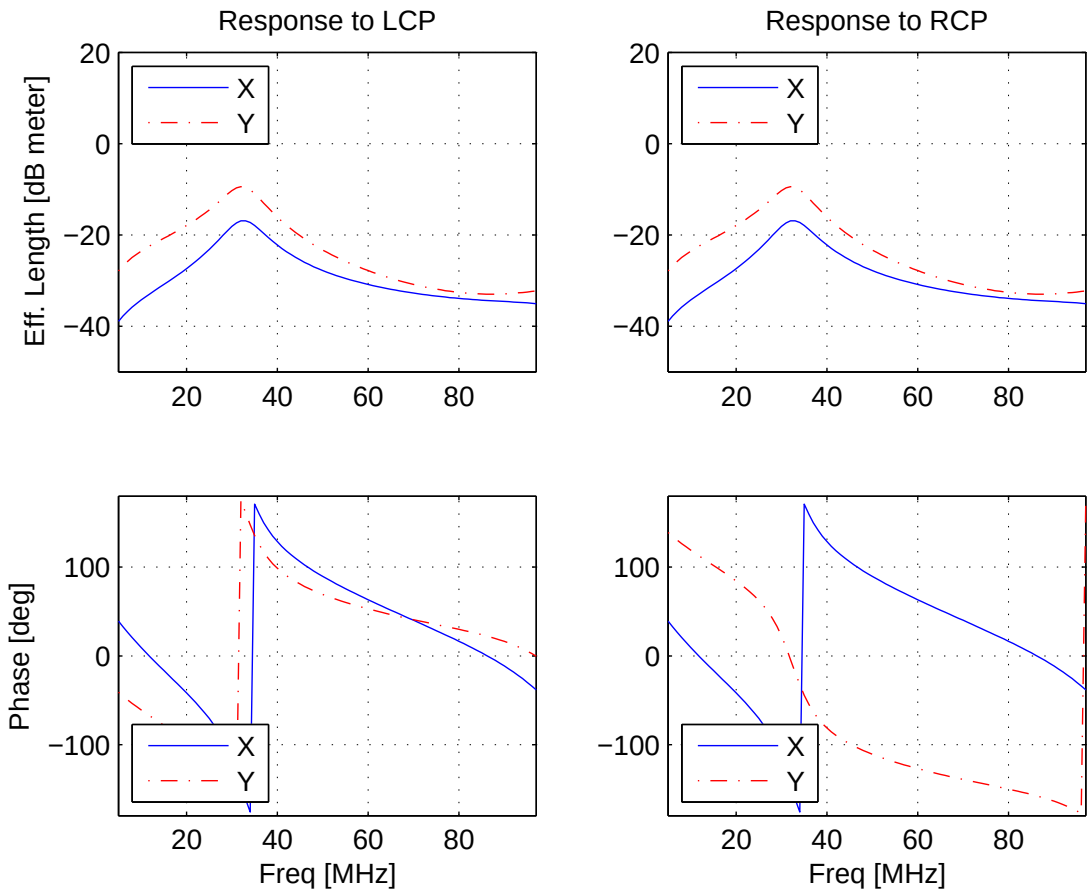

Figure 8: $\theta = 74°$, $\phi = 0$, standalone stand.

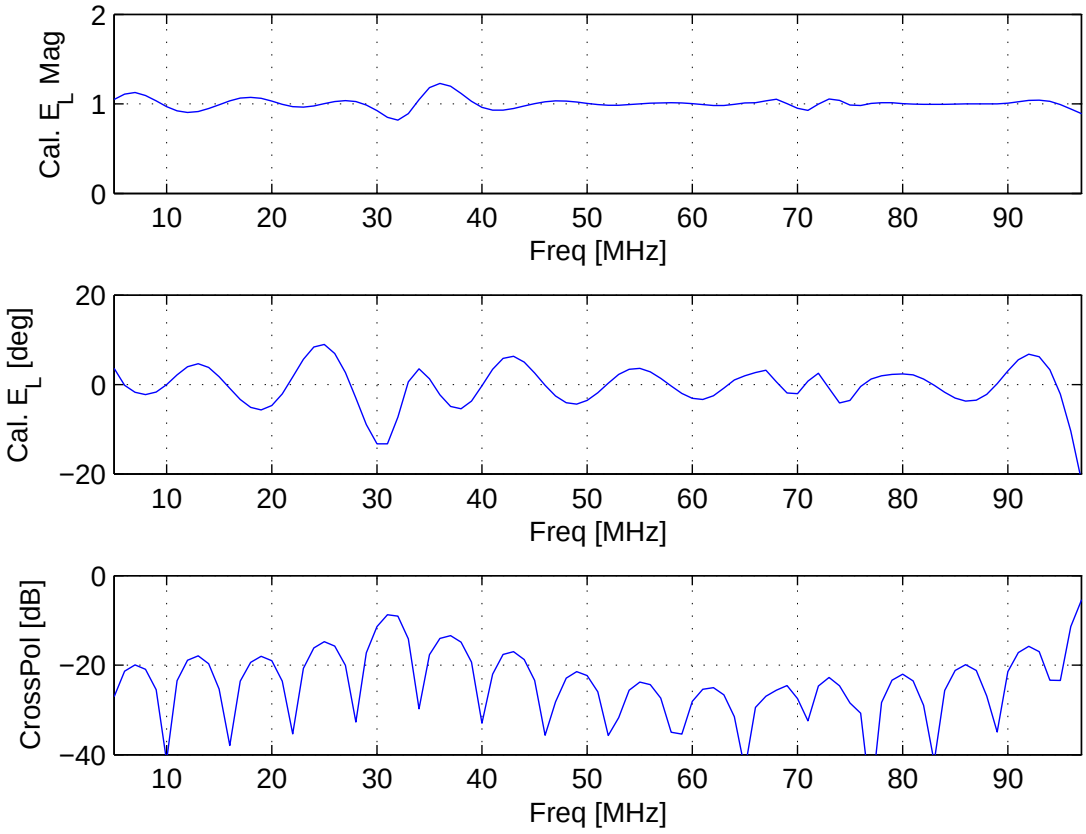

Figure 9: $\theta = 74°$, $\phi = 0$, embedded stand.

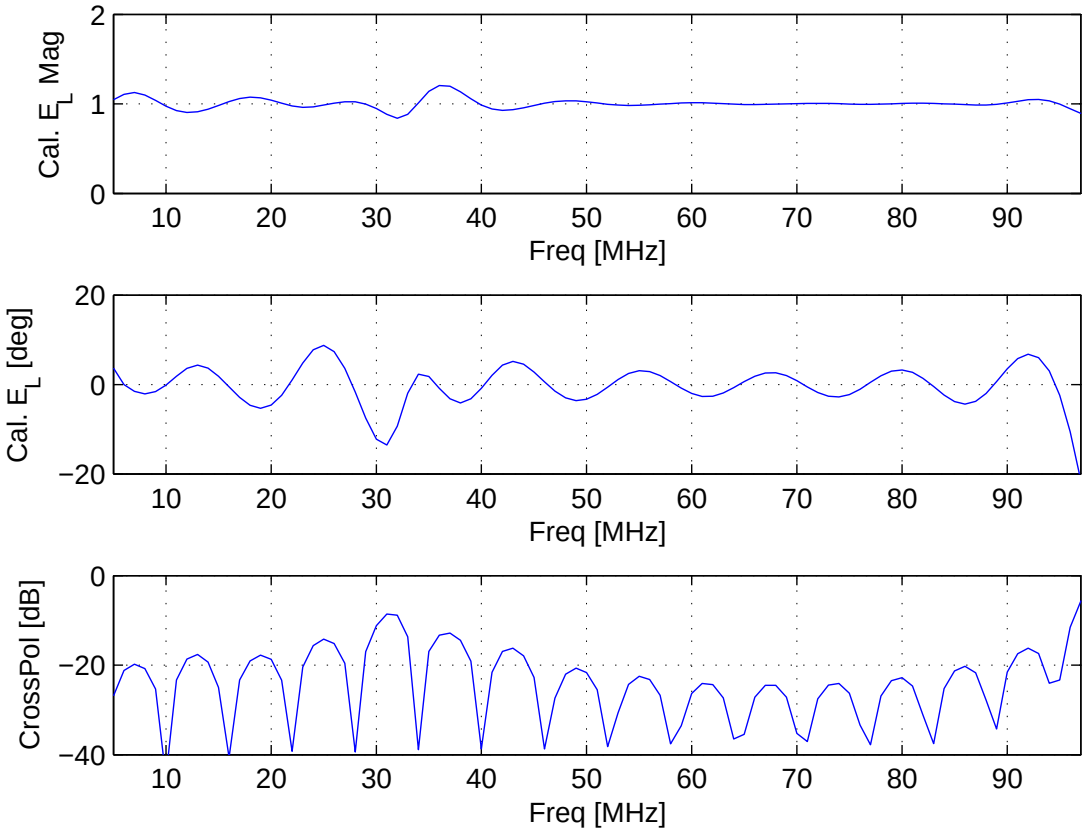

Figure 10: $\theta = 74°$, $\phi = 0$, standalone stand.

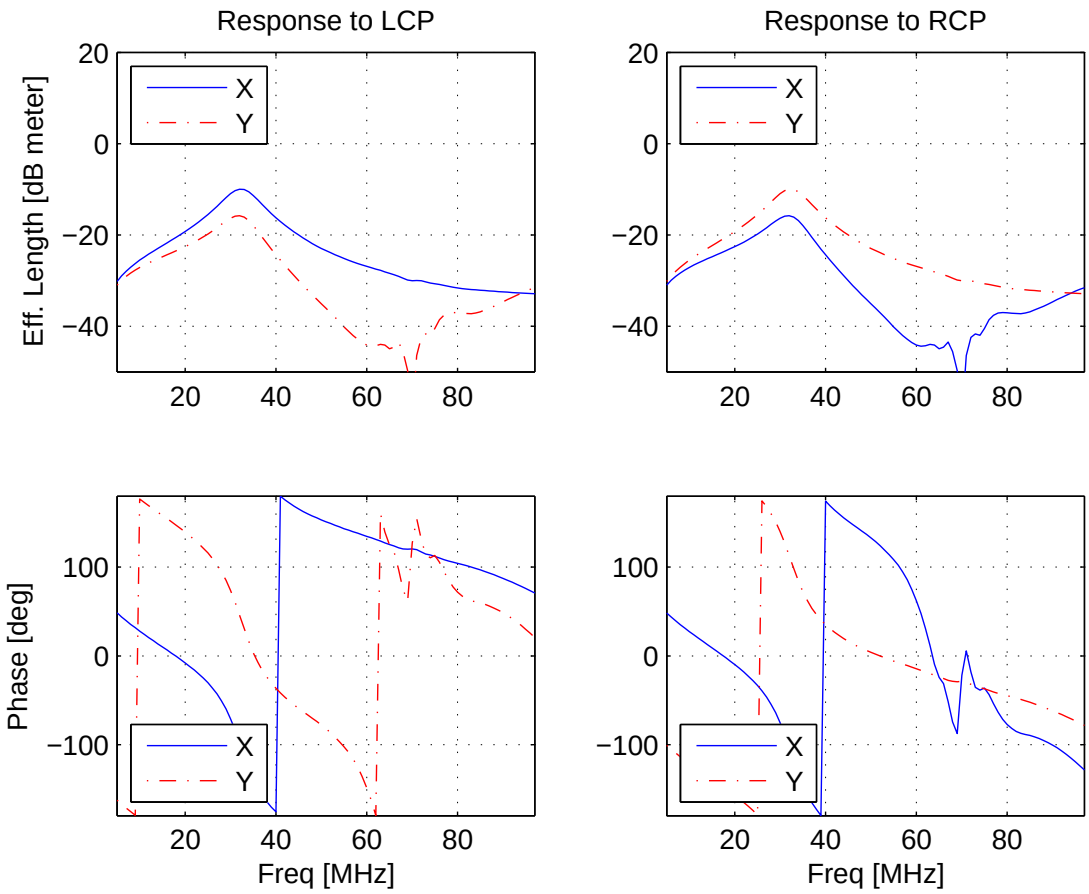

Figure 11: $\theta = 74°$, $\phi = 45°$, embedded stand.

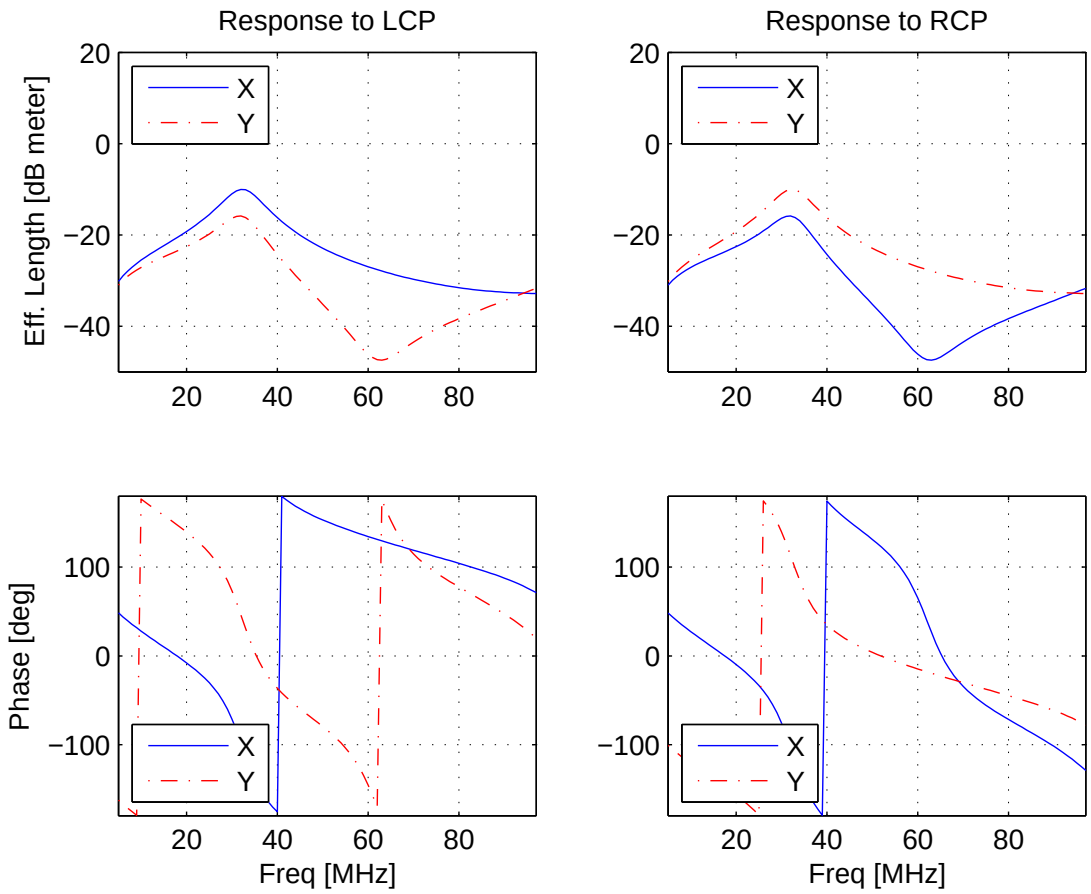

Figure 12: $\theta = 74°$, $\phi = 45°$, standalone stand.

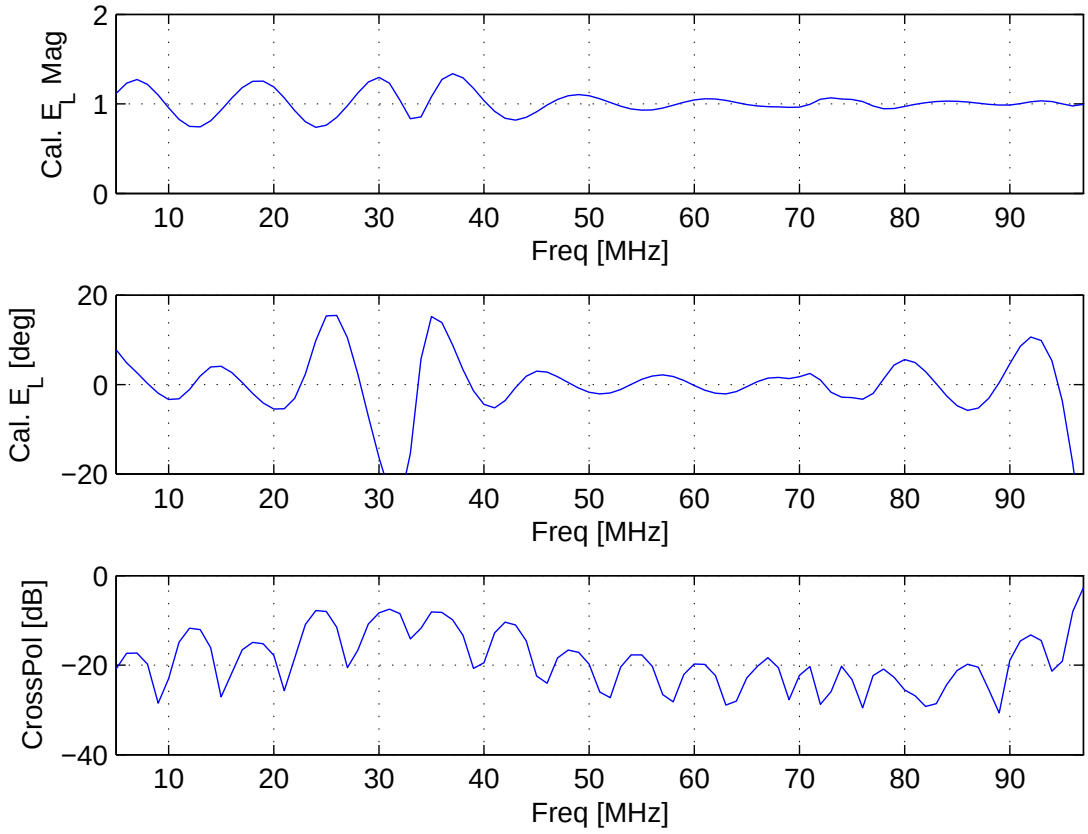

Figure 13: $\theta = 74°$, $\phi = 45°$, embedded stand.

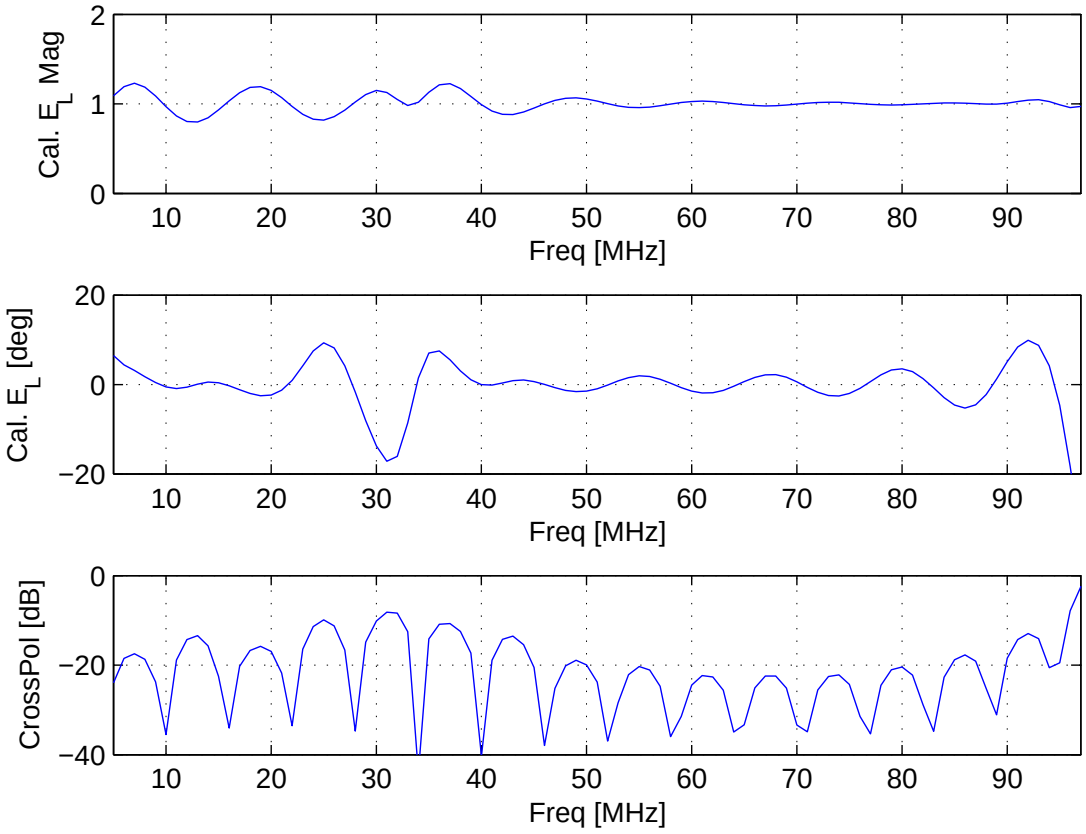

Figure 14: $\theta = 74°$, $\phi = 45°$, standalone stand.

References

[1] S. Ellingson, "Single-Stand Polarimetric Response and Calibration," Long Wavelength Array Memo Series No. 138, June 15, 2008. [online] http://www.phys.unm.edu/∼lwa/memos.